ELSEVIER

Journal of Marine Systems 37 (2002) 17–29

JOURNAL OF MARINE SYSTEMS

www.elsevier.com/locate/jmarsys

Observations of the creation and evolution of small-scale oceanic frontal cusps and slicks

George Marmorino*, Farid Askari[1], Richard Mied

Naval Research Laboratory, Remote Sensing Division, Washington, DC 20375-5351, USA

Received 2 November 2000; received in revised form 19 June 2001; accepted 19 June 2001

Abstract

Airborne microwave radar imagery and coincident in situ data collected off Cape Hatteras, NC (USA) are used to examine the small-scale horizontal structure of a frontal region, which formed through intrusion of relatively dense Gulf Stream water onto the continental shelf. The frontal outcrop is shown to have a kilometer-wavelength scalloped structure consisting of sharp angular features (cusps) alternating with broad, gently curved regions (troughs). There is also an associated pattern of slicks lying on the buoyant side of the front and asymmetrically offset from the cusps. These slicks appear to originate from biophysical processes associated with the front itself and to trace out cyclonic trajectories of surface fluid particles. It is conjectured that the distinctive horizontal pattern of frontal cusps and slicks arises from shear-flow instability modified by the requirement for convergence of buoyant water along the front.

Subject keywords: Gulf Stream intrusion, Ocean front, Frontal instability, Shear instability, Current convergence, Frontal convergence, Ocean slick, Surfactant, Imaging radar
Regional terms: USA, North Carolina, Cape Hatteras, Gulf Stream

1. Introduction

A peculiar but common feature associated with the surface expression of an ocean front is the occurrence of a scalloped pattern consisting of alternating cusps and troughs. That is, the planform of the frontal outcrop exhibits sharp angular features (cusps) in between broad, gently curved regions (troughs). Examples have been seen along the edge of the outflow from the Connecticut River into the Long Island Sound (Garvine and Monk, 1974; see review by Largier, 1992); along a tidal front in the English Channel (Pingree et al., 1974); and recently over the inner continental shelf near the mouth of the Chesapeake Bay (Sletten et al., 1999). These are small-scale features having a cusp-to-cusp wavelength of the order of 100 m to about 1 km. Their ecological significance is unknown, nor is it known what clues their structure may hold for diagnosing any physical characteristics of the frontal region. Published observations showing their temporal development are nonexistent.

* Corresponding author. Tel.: +1-202-767-3756; fax: +1-202-767-3303.
E-mail address: marmorino@nrl.navy.mil (G. Marmorino).
[1] Present affiliation: Saclant Undersea Research Center, La Spezia, Italy.

0924-7963/02/$ - see front matter
PII: S0924-7963(02)00193-8

In this paper, we examine a unique set of observations that shows the creation and evolution of a series of small-scale cusps along a shallow ocean front near Cape Hatteras, NC (Fig. 1). This front forms through incursion of relatively dense Gulf Stream-type water onto the shallow continental shelf (e.g., Mied et al., 1996; Churchill and Berger, 1998). The data set consists of a 2-h-long sequence of microwave radar images of the sea surface, which were collected aboard an aircraft, and simultaneous near-surface hydrographic measurements and sea-surface video imagery, which were collected aboard a research ship. An additional aspect is the observation of surfactant slicks that appear to be spawned and advected by the frontal circulation and so form a spatial pattern complementary to that of the frontal cusps. While the data are limited, we attempt to synthesize the observations into a conceptual model of the three-dimensional flow of an unstable front.

2. Background

2.1. Previous work

Aspects of the front have been reported previously by Marmorino and Trump (1994). They described it as follows: "At sea, the front between Gulf Stream water and shelf water was unmistakable. It was delineated by a narrow band of short, pyramidally shaped surface waves; an adjacent zone of *Sargassum* weed and floating debris; an audible gurgling (presumably from small-scale wave breaking); a color change from green on the north side to blue on the south; a distinctly corrugated structure on many scales with sharp cusps pointed northward; and finally, an impression of relative motion through the ambient sea." While the intruding Gulf Stream water was denser than the shelf water, it was nevertheless about 2 °C warmer and so a satellite infrared image showed

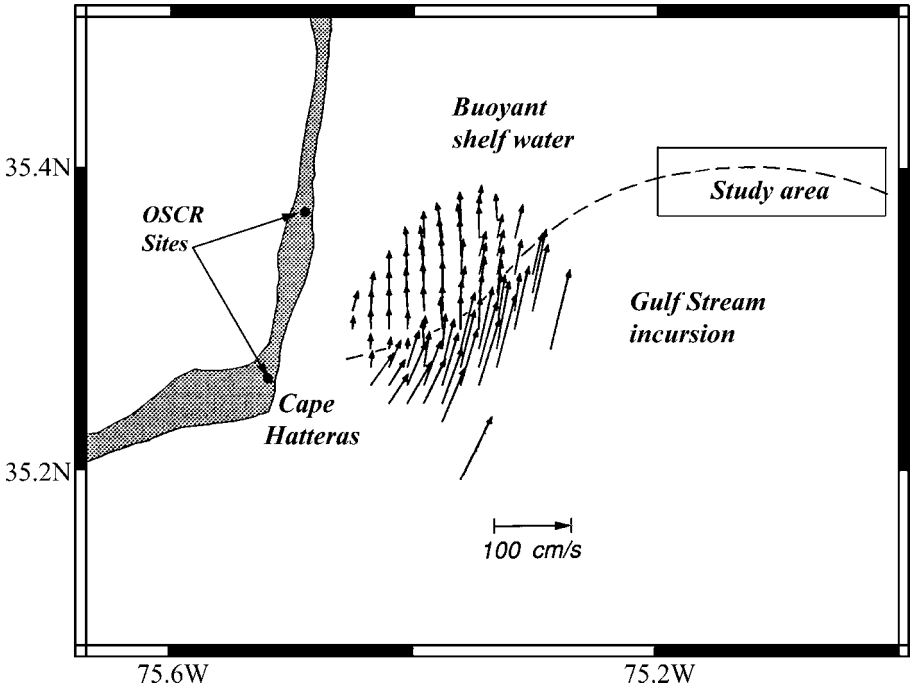

Fig. 1. Location of study. Dashed curve indicates frontal position as determined from an AVHRR image acquired at 1528 LT 17 September 1991. The frontal orientation in the study area (rectangle) is approximately east–west. Vectors are surface currents measured at 1520 LT using the University of Miami's Ocean Surface Current Radar (OSCR), which has a spatial resolution of about 1 km. (Figure modified from Marmorino and Trump, 1994.)

the full across-shelf extent of the front (Fig. 1, dashed curve). The frontal orientation was approximately east–west over the middle shelf (water depth of about 30 m), which is the area of interest in the present paper. Fig. 1 also shows a representative snapshot of the surface flow field near Cape Hatteras as reported by Chemi et al. (1993). South of the front, the flow is seen to be about 70 cm/s toward the north–northeast, but it changes abruptly across the front to a weaker (about 30 cm/s) northward flow in the shelf water. Thus, there is both an across-front current convergence and a cyclonic along-front shear. The Rossby number for the flow can be estimated as $Ro = \Delta u/\Delta y f \approx O(5)$, where $\Delta u \approx 40$ cm/s is the change in along-front velocity, $f = 8.4 \times 10^{-5}$ s^{-1} is the local value of the Coriolis parameter, and $\Delta y \approx 1$ km is the approximate north–south width of the velocity front.

Motivated by these observations, Mied et al. (1996) investigated a mechanism for frontogenesis. They found that over a range of plausible initial configurations for the shelf and Gulf Stream water masses, the flow evolved to produce a propagating gravity current whose surface expression is a strongly convergent front. Computation of the convergent current field in the across-front plane was used by Jansen et al. (1998) to provide input to a wave–current interaction model, the output from which was used to model the variation in radar backscatter across the front. Numerical simulations of the backscattered signal from a convergent front assumed to have a sinusoidal surface shape were subsequently performed by Chubb et al. (1999).

2.2. Radar measurements

The radar measurements were made using an X-band (9.375-GHz frequency), horizontally polarized, real-aperture radar (RAR), which was flown aboard a Naval Research Laboratory P-3 aircraft. The mean incidence angle of the measurements was 45°, so the radar was Bragg-resonant with surface waves having a wavelength $\lambda_B = 2.3$ cm (Bragg wave number $k_B = 278$ rad/m). On 17 September 1991, from 1310 to 1504 LT (local time refers to Eastern Daylight Time), the aircraft flew 12 alternating eastward and westward passes (hereafter Passes 1 through 12) along the front described above. Each pass extended from approximately 75.0–75.2°W, a distance of about 15 km (Fig. 1). In this paper, we focus on imagery of the middle-section of the front, which contained the best examples of the cusps and related slicks. An image showing our Pass 10 in its entirety appears in Jansen et al. (1998) as Plate 1. The spatial resolution of the radar measurements is 11 m in the range (approximately across-front) direction but 30 to 50 m in the azimuth (along-front) direction depending on the altitude of the aircraft, which varied between 900 and 1800 m. A shortcoming of the measurements is the inability to precisely register the imagery because of a large drift rate (nearly 2 km/h) in the inertial navigation system used aboard the aircraft.

2.3. In situ measurements

Shipboard data were collected both during and after the radar measurements. Continuous hydrographic measurements were made using towed conductivity and temperature sensors. Only those data collected from 1737 to 2138 LT (i.e., 2.5 to 6.5 h after the radar measurements were made) were analyzed by Marmorino and Trump (1994). They found that the sensors at 5.3-m depth showed no density front (their Fig. 5) while the sensors at 4-m depth caught only the lowest part of the density interface (their Fig. 7). Only the shallowest available sensor (at 2.4 m) showed a strong density jump along the frontal outcrop line (their Fig. 4). Thus, the buoyant layer of shelf water layer near the front was rather shallow. We confirmed their results for the period of the RAR measurements through a separate examination of the towed data (not shown). Therefore, in the present paper, we will use data from the 2.4-m depth conductivity sensor, which has a horizontal resolution of about 0.5 m, to examine horizontal variability in the density field, which is dominated by changes in salinity. As conductivity is proportional to salinity, the data from this sensor adequately portray the changes in density while also showing some features of interest because of an additional dependence on temperature.

Shipboard acoustic Doppler current profiler measurements were also collected, but the 7-m depth of the shallowest sample bin renders them of little value in the present study. We have, however, made extensive use of time-encoded video recordings of the sea surface that were made from the bow of the ship. While these recordings are used here in only a qualitative

way, Marmorino et al. (1999) present a quantitative analysis of related sea-surface features found near the study area on 16 September (the previous day). Winds recorded aboard the ship and at a nearby buoy at the time of the radar measurements were light (about 3 m/s) and from the south.

3. Observations

3.1. Radar imagery of the frontal outcrop line

Fig. 2 shows subscenes from Passes 1, 6, 10, and 12 that cover approximately the same 7-km-long section of the frontal region (see Table 1 for details of the data collection for these passes). The frontal signature is the continuous lightly shaded curve; white represents the highest measured values of radar backscatter. Individual data slices across the frontal signature shows it has a width of about 50 m and an intensity at least 10 dB higher than background signal levels. Such a large X-band signal is predicted at a convergent front by models that include the effects of intermediate-scale breaking waves (Jansen et al., 1998; Lyzenga, 1998).

A number of frontal cusps appear in the images, the clearest being numbered as 1 through 6. Each of the cusps points northward into the shelf water and

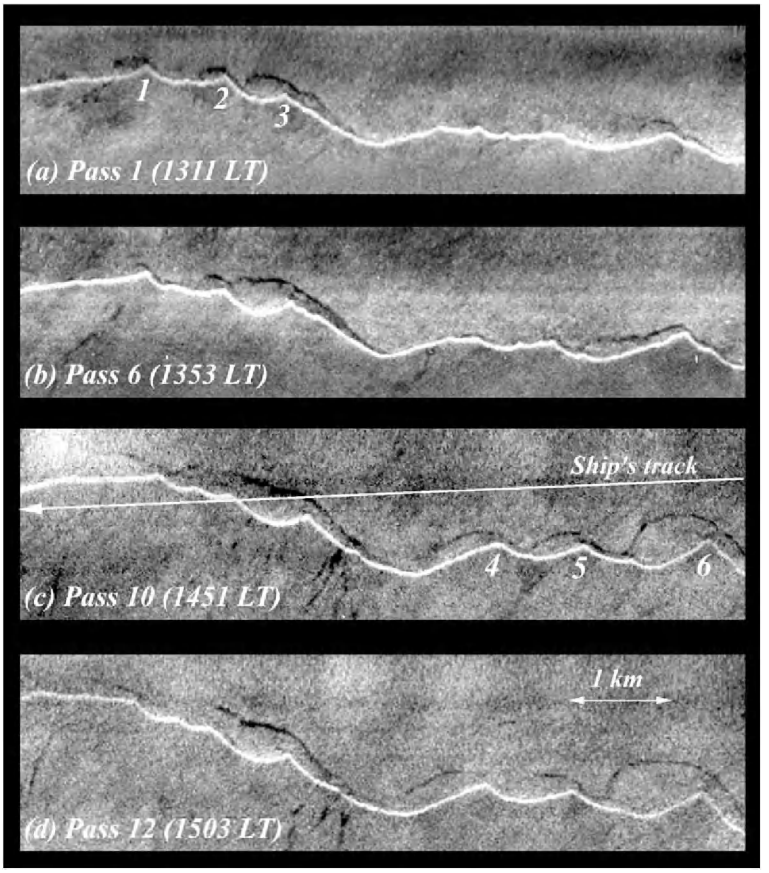

Fig. 2. Subscenes from radar Passes 1, 6, 10, and 12. The images extend in longitude from about 75°3′W to 75°7′W, or about 7 km. Whiter (blacker) shades indicate regions of relatively higher (lower) radar backscatter. The continuous white curve represents the frontal outcrop line, which is deformed into a scalloped pattern containing six prominent cusps (1–6). Narrow black regions represent surfactant slicks. Horizontal banding in the images is an artifact and should be ignored. Line superimposed on the Pass 10 image shows the track of the research vessel from about 1400 to 1440 LT.

Table 1
Details of data collection for the radar scenes shown in Fig. 2

Identification	Aircraft		Resolution		Incidence angles	File name	Acquisition time (EDT)
	Altitude (m)	Heading (°T)	Range (m)	Azimuth (m)			
Pass 1	914	271	11	28	34–59°	RAR014	1310:56
Pass 6	1828	271	11	46	30–55°	RAR020	1353:11
Pass 10	1859	275	11	47	37–51°	RAR027	1451:30
Pass 12	1859	275	11	46	30–54°	RAR029	1503:34

has an inclusion angle of about 120°. Cusps 1–3, which appear in the western half of the images, have a wavelength of about 700 m. The north–south distance between a cusp and an adjacent trough gives an amplitude of about 100 m. While cusps 1–3 persist, subtle changes occur such as the growth of a new cusp located between cusps 1 and 2. Further evidence of frontal evolution can be seen in the eastern half of the images where initially (Pass 1) there appear many randomly spaced small-amplitude corrugations, some having a wavelength as small as 100 to 120 m, as well as the early development of cusp 6. Cusps 4 and 5 begin to take shape by Pass 6. By Pass 10, each of the cusps 4, 5, and 6, has grown to large amplitude (100 to 200 m) and a wavelength of 800 m to 1.2 km. Therefore, while cusps having a range of spatial scales may appear initially, a dominant scalloped pattern quickly emerges having a roughly constant wavelength and amplitude, which persists over at least several hours.

3.2. Slicks in the radar imagery

In addition to the high-backscatter frontal signature, the radar images show narrow low-backscatter features (i.e., the more darkly shaded and black areas in Fig. 2) occurring in both the shelf water and Gulf Stream. Data slices made across the more distinct of these features show a signal of about 10 dB below ambient levels. This reduction in radar signal is consistent with damping of the Bragg-resonant surface waves by a film (or slick) of biogenic surface-active (surfactant) material. The extent of the wave damping can be estimated using an equilibrium wave spectrum model and an in situ film elasticity measurement of about 25 mN/m made nearby but on the previous day (Marmorino et al., 1999). For the measured wind speed of about 3 m/s and an X-band Bragg wave number $k_B = 278$ rad/m (Section 2.2), Marmorino et al.'s Fig. B2 shows a damping of about 9.5 dB, which is indeed comparable to the present radar measurements.

The most prominent and persistent slicks occur in the shelf water in association with the cuspy parts of the front. These slicks tend to lie nearest the front east of a cusp and extend progressively farther from the front to the west of a cusp except that they often reattach to the front (or, to another slick lying near the front) just eastward of the next cusp in the series. Thus, each cusp appears to have a companion slick that is spatially fixed to it in a recurring pattern, though this pattern can evolve somewhat over time. For example, the slicks associated with cusps 1–3 appear to merge over time and to move farther from the front. Similarly, the slicks associated with cusps 4–6 develop over time, growing roughly on the same time scale as the cusps (see below). Note in particular the close similarity between the more newly formed slick patterns in the final pass for cusps 4–6 (Fig. 2d) and the pattern for cusps 1–3 in the first available pass (Fig. 2a). It is interesting that these frontally offset slicks persist over the measurement period as dynamical arguments suggest there should be a surface flow of buoyant shelf water converging on the front (Garvine, 1974, 1979). Therefore, one would expect slicks on the shelf-water side of the front to advect into the front over the observation period.

Slicks occurring south of the front in the Gulf Stream water, on the other hand, bear no apparent relationship to the pattern of frontal cusps. Rather, they appear similar to a set of Gulf Stream slicks observed in synthetic aperture radar (SAR) images acquired on the previous day in about the same area and analyzed by Lyzenga and Marmorino (1998). These authors were able to measure the displacement of distinguishing features in slicks between two successive SAR images spaced 20 min apart, which they then used to infer surface currents (and current gra-

dients) that compared well with simultaneous shipboard current measurements. Similarly, we were able to track those Gulf Stream slicks appearing in multiple passes. While a few of these slicks had the occasional odd shape, the vast majority were quasi-linear and aligned north–northeastward (approximately in the Gulf Stream flow and wind directions); all were observed to move into the front over time and then disappear from view. This provided several independent estimates of the surface current in the Gulf Stream water. Measured relative to the front, this flow was northeastward at 15 to 35 cm/s (a relative eastward flow of 11 to 25 cm/s), which is consistent with Marmorino and Trump's (1994) ADCP measurements made on the Gulf Stream side of the front.

The slicks occurring in the shelf water and associated with the evolving cusps could also be tracked over time. As an example, Fig. 3 shows details of the region near cusp 6 for Passes 1 to 6. The figure shows the evolution of the scene at 6- to 13-min intervals over a total period of 42 min. Initially, in Pass 1, a slick extends along the eastern side of the cusp and curves cyclonically around the cusp, while in Pass 3 the slick appears to have straightened out west of the cusp. This suggests variability on more than one length scale as might be expected during a transient developmental stage. Passes 2 through 6 show a continuing elongation of the slick toward the west. The time series deteriorates after Pass 6 with Pass 7 (not shown) occurring 31 min later and then cusp 6 not being seen clearly again until Pass 10 (Fig. 2c), which shows an increased northerly separation between the slick and frontal outcrop. Tracking the position of the very westward end of the slick over Passes 1 to 6 gives a speed of about 20 cm/s, which can be taken as an estimate of the surface flow in the shelf water measured relative to the front. This relative westward flow as inferred from the imagery would be compatible with maps of surface currents shown in Fig. 1 only if the cusps themselves moved eastward. That this was the case shown by Marmorino and Trump (1994) who referenced their in situ sampling to a particular cusp that moved over a 3-h period towards 38°T at mean speed of 41 cm/s (their Section 5.1). The relative flow in the shelf water can be combined with that inferred above on the Gulf Stream side to give an across-front cyclonic shear flow of $\Delta u \approx 40$ cm/s, which is consistent with the estimate made in Section 2.1.

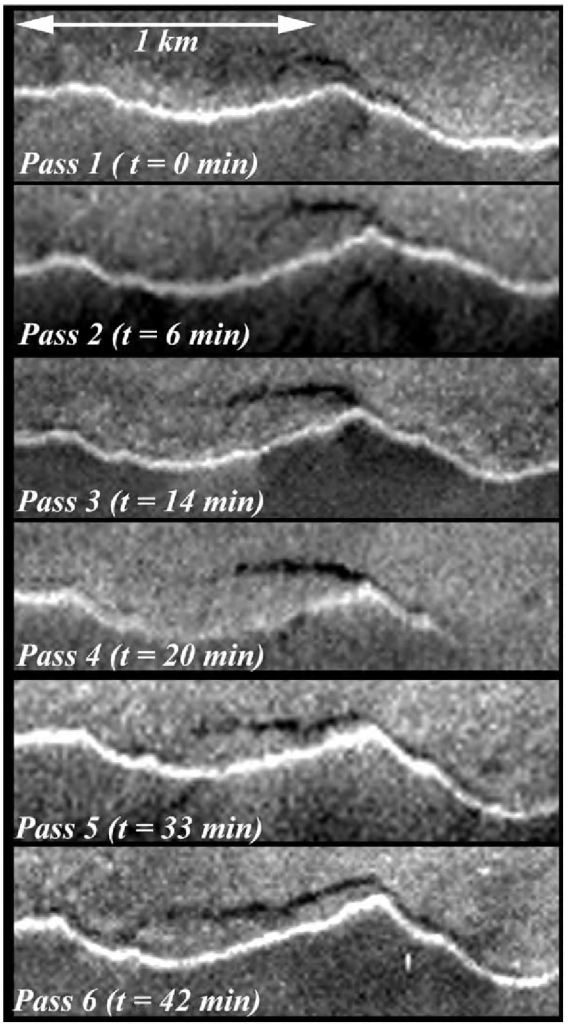

Fig. 3. Subscenes from radar Passes 1–6, showing details of the evolution of cusp 6 and adjacent slick.

3.3. Shipboard video measurements of the sea surface

The surface expressions of several of the features appearing in the radar imagery were recorded by video cameras aboard the research ship as it sailed westward across the area shown in Fig. 2 from about 1400 to 1440 LT. The ship's track relative to the frontal features is indicated on the Pass 10 radar image (Fig. 2c; 1451 LT) and was determined by closely examining the radar imagery for the signature of the ship and its wake as well as by examining the wide-

view video imagery. It can be seen that the ship passed north of cusp 3 and then intersected a slick between cusps 2 and 3. Taking the relative crossing angle into account and using a ship's speed of 2.1 m/s, the width of the slick was estimated from the video data to be about 35 m, or about three times the range resolution of the radar. The slick itself was nondescript having indistinct edges marked by neither weed nor foam. As the ship continued westward, a second slick was observed in the video imagery within about 40 m of the front. The width of this slick was roughly comparable to the range resolution of the radar and so it is marginally resolved in the radar imagery as a faint dark line just east of cusp 2 (Fig. 2c). The edge of the slick was marked by masses of foam (Fig. 4a), which points to a biogenic origin. Foam is expected to also appear dark to an X-band RAR (Alpers et al., 1981). Such an accumulation of foam through surface convergence might have been expected to occur immediately along the frontal outcrop (Le Fevre, 1986). Between the foam band and the front, the video data showed pieces of *Sargassum* weed present primarily in great masses along the Gulf Stream side of the front (Section 2.1).

A second video image (Fig. 4b) reveals something of the nature of the sea surface that is responsible for the bright radar signature of the front. Appearing in the upper left of the figure is the highly regular pattern of short waves (wavelengths the order of 30 cm) referred to as pyramidal waves in Section 2.1. These waves are thought to delineate the frontal outcrop line. The middle part of the figure shows intermediate-scale waves (wavelengths the order of 2 m) that have propagated through the frontal outcrop region to break in the shelf water. The occurrence of such a region of breaking waves downwind of the frontal convergence is consistent with predictions of wave–current interaction models (e.g., Jansen et al., 1998; Lyzenga, 1998). The length of wave crest breaking in this region was investigated separately using the video data and found to vary from 0.5 to 2.5 m, with 1 m being the most common value (Kaiser, personal communication, 1998).

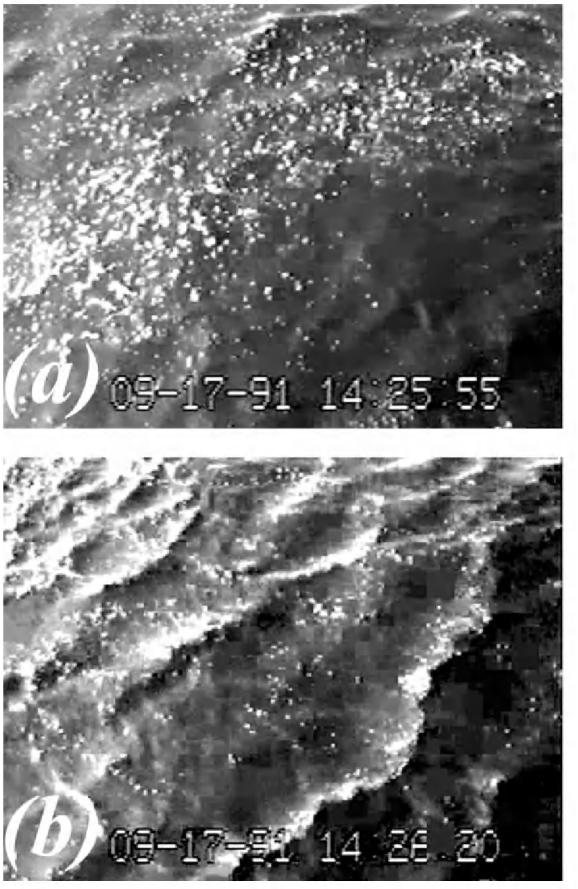

Fig. 4. Video frames showing surface conditions near cusp 2. Each frame shows an approximately 5 × 4 m area of the sea surface. View is westward toward the top of the page. (a) Image at 1425:55 LT shows large accumulations of surface foam along the northeast edge of a slick located about 40 m from the front. (b) Image at 1426:20 LT shows breaking waves downstream of the frontal outcrop that result from wave–current interaction.

3.4. Near-surface hydrography

The hydrographic data collected during the airplane flights were examined with reference to both the radar and shipboard video imagery. An illuminating sample of data comes from the single occasion when the towed sensors passed cleanly through both sides (i.e., east and west sides) of a cusp. This occurred about 2 km west of the scene shown in Fig. 2 and unfortunately the associated surfactant-related structure apparent in the video recordings (see below) is not resolved in the radar image, which is therefore not shown; however, there are close similarities to the transect made near cusp 2, for which a radar image is shown in Fig. 2c. Fig. 5a shows a schematic of the sampling across the cusp, and Fig. 5b shows the data

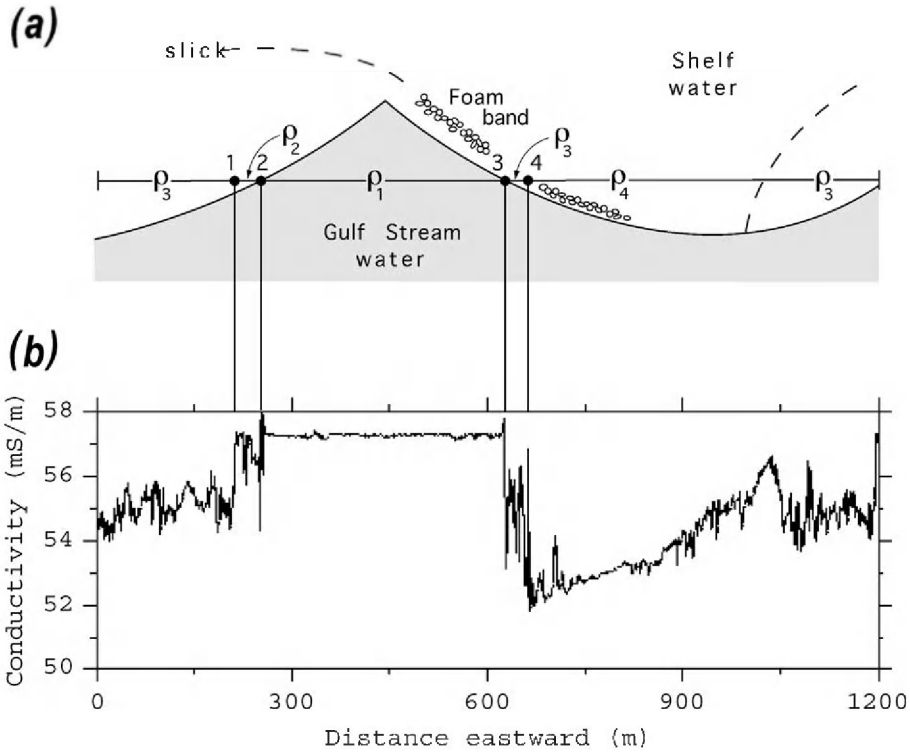

Fig. 5. Transect through a frontal cusp. (a) Interpretative sketch showing the sensor path (horizontal line) relative to the frontal outcrop (solid curve), foam band (small circles), and slicks (dashed curves). Numbers indicate front-crossing positions; different water 'types' are indicated by density values ρ_1 through ρ_4. Foam line and slick positions relative to the frontal cusp were estimated from shipboard video recordings but structure is qualitatively similar to that shown in Fig. 2c, just east of cusp 2. (b) Data from a conductivity sensor towed at a mean depth of 2.4 m from 1438:30 to 1448:00 LT.

from the conductivity sensor at 2.4-m depth. The water lying within the cusp (denoted in the figure as water of density ρ_1) represents the high-salinity water on the Gulf Stream side of the front. This water is nearly homogeneous but for two peaks in the conductivity trace near the frontal outcrop (identified by 2 and 3 in the figure). We believe these peaks indicate diurnally warmed surface Gulf Stream water that has been subducted to the depth of the sensor. The freshest shelf water in the record (water density ρ_4) occurs east of the cusp but is separated from the outcrop by a secondary front (4). This front coincides with a narrow foam band (width estimated from the video data to be about 4 m). Between the foam band and the outcrop line, the trace shows widely fluctuating values and so we identify this as a mixing region having mean density ρ_3, where ρ_3 is approximately midway between ρ_1 and ρ_4. The width of this region of ρ_3 water is, after taking account of the sampling geometry, about 30 m perpendicular to the front. A qualitatively identical conductivity trace and a similar width of a ρ_3-water mixing region occur for the transect made just east of cusp 2. Toward the right-hand side of the figure, the trace shows values gradually increasing to about the level of ρ_3 and the video record shows a narrow slick and an adjacent area of rougher water suggesting a region of wave–current interaction. On the left-hand side of the figure, another secondary front (1) occurs near the outcrop. This front has a relatively small density jump and no associated foam band in the video recording. The water lying between this secondary front and the outcrop (a width now of about 15 m) is identified as mixed fluid of density ρ_2, where $\rho_3 < \rho_2 < \rho_1$. A complementary view of the across-front structure located about 400 m west of the cusp shown in Fig.

5 (but 3 h later) appears in Marmorino and Trump's (1994) Fig. 7a, which indicates both an outcrop and secondary front.

The interpretation of the hydrographic measurements is aided by reference to Fig. 6, which sketches an idealized vertical section across a shallow, convergent front. We can imagine this section being made at a position just east of the cusp shown in Fig. 5a. The surface outcrop and frontal interface are indicated in Fig. 6 by the upturning ρ_1 isopycnal and would thus correspond to front 3 in Fig. 5. A rotor-like circulation is indicated in the 'head' region of the front, as suggested by velocity measurements made across plume fronts (Luketina and Imberger, 1987; Marmorino and Trump, 2000). Large vertical shear in the head is expected to create flow instabilities and large fluctuations in density as the dense ρ_1 water begins to mix with the inflowing layer of buoyant ρ_4 water. The sensor in Fig. 5 is assumed to lie shallow enough to sample this buoyant layer. Evidence of this mixing is provided by the large conductivity fluctuations shown in Fig. 5b. A shoaling ρ_3 isopycnal in Fig. 6 indicates a secondary front near the trailing edge of the rotor. Evidence for such a trailing-edge density front can be seen in the laboratory shadowgraphs made by Britter and Simpson (1978) (their Fig. 1b); also, the field observations sometimes show secondary frontal density structure occurring near the trailing-edge of the rotor (though they have not been interpreted in this way before). We thus identify front 4 in Fig. 5 with a trailing-edge front. Similarly, fronts 1 and 2 on the west side of the cusp in Fig. 5 would correspond to trailing- and leading-edge fronts. The solid curve in Fig. 6 indicates the zero isotach for the relative flow (c.f., Liu and Moncrieff, 2000). The abrupt deepening of this isotach near the trailing edge of the rotor indicates horizontal convergence. Evidence for this convergence is the occurrence of the foam band along the trailing-edge front 4 in Fig. 5. Other factors may explain why a foam band was not observed along front 1. These include a more weakly developed frontal head as the result of the more acute angle between the front and the inflowing dense water, as well as the pattern of the larger-scale fluid circulation (see below).

3.5. Synthesis

We can now attempt a synthesis of the radar and in situ observations. Fig. 7 shows a plan view of the frontal region including a sketch of the surface relative flow field. The background flow relative to the

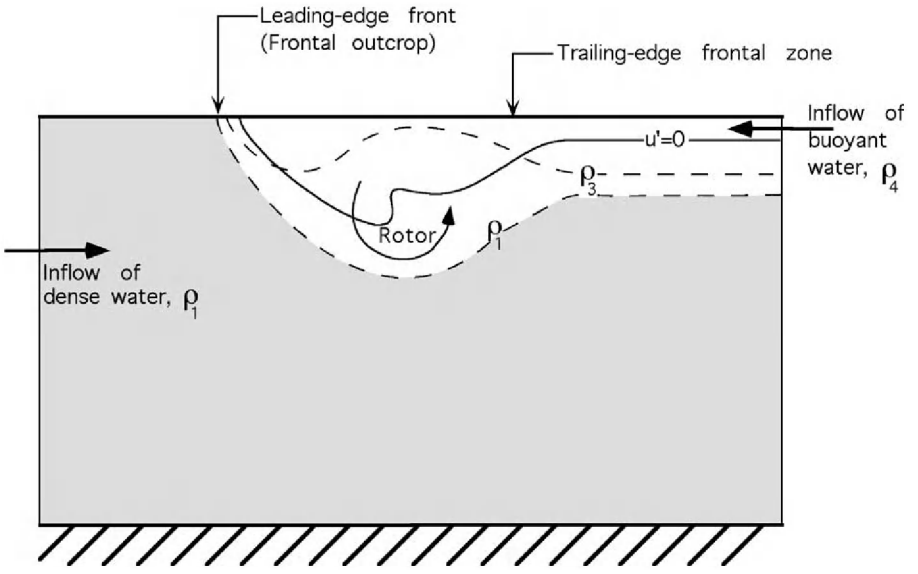

Fig. 6. Schematic vertical section made across the front at a position just east of a frontal cusp. Vectors indicate flow measured in a reference frame fixed to the frontal outcrop, the solid curve indicates the $u'=0$ isotach. Dashed curves are isopycnals.

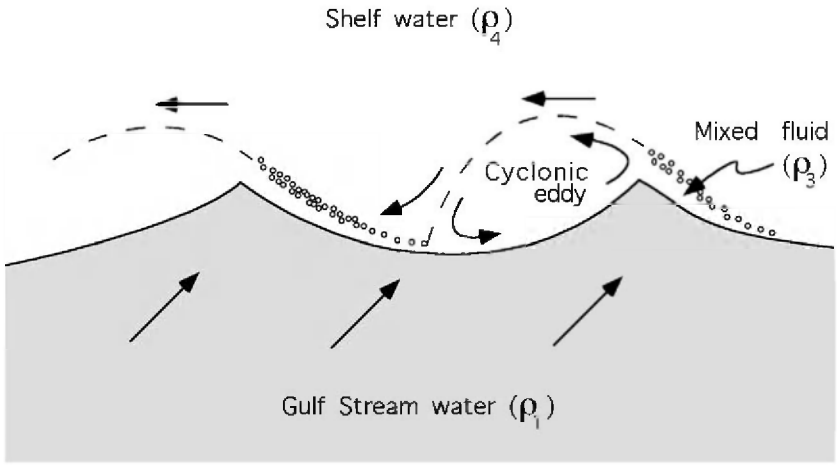

Fig. 7. Plan view of frontal region. Details in the velocity field (indicated by the arrows) are conjectural.

front is northeastward in the Gulf Stream water (shown as density ρ_1) and westward in the shelf water (density ρ_4). Nearer the front, however, the flow on the shelf waterside is assumed to be perturbed by a flow instability, the nature of which is discussed in the next section. As a result, the flow downstream of a cusp reverses direction, creating a cyclonic eddy, while the flow upstream of a cusp turns southwestward and toward the front. It is thus on the upstream side of a cusp that the most buoyant shelf water (density ρ_4) is found, resulting in a large density contrast ($\Delta\rho = \rho_3 - \rho_4$) across the trailing-edge front there. The cyclonic eddy, however, diverts the ρ_4 water; thus, water within the cyclonic eddy is assumed to derive instead from the upstream rotor-mixing region and to have a density approximately equal to ρ_3. In the imagery, therefore, a slick on the upstream side of a cusp is assumed to delineate the trailing-edge front, i.e., the transition from shelf water of density ρ_4 to mixed fluid of density ρ_3. The imagery shows that the distance between the outcrop and upstream slick increases toward the cusp. Thus, the region of mixed fluid thickens in the downstream direction as an accumulated inflow of shelf water, akin to a growing boundary layer. The downstream slick is presumed to derive primarily from cyclonic advection of surfactant from the upstream foam band. The evidence for the asymmetry in the flow field sketched in Fig. 7 is, thus, the asymmetry in slick positions in the radar images, the asymmetry in the measured density field, and the asymmetry in the location of foam bands.

4. Discussion

In the previous section, we have assumed that the large-scale patterns observed in the data arise from the occurrence of a hydrodynamic instability. The possible nature of this instability is discussed in the present section. Calculations on the instability of a geostropically balanced front having isopycnals that outcrop at the surface have been performed by Samelson (1993), Wang (1993), and Samelson and Chapman (1995), who show that the most unstable mode of instability has a growth time of 2 to 3 days and a wavelength of about 70 km, comparable to 2π times the internal radius of deformation L_o. By comparison, the patterns we observe have a wavelength of about 1 km, or only about one-fourth the value of L_o as calculated by Marmorino and Trump (1994), and they grow to finite amplitude in about 1 h. These relatively small length and time scales suggest the baroclinic instability mechanism is not directly applicable to our observations.

Recently, Munk et al. (2000) have proposed a conceptual instability model that combines a baroclinic growth phase and a barotropic instability phase. The submesoscale 'spiral eddy' structures they

attempt to explain have large wavelengths of the order of 20 km, but their model is of interest because it assumes that a horizontal shear instability develops along the cyclonic side of a frontal flow if, as in our case, the Rossby number is greater than one. However, a difference arises in our case because of the similarity to the dynamics of a gravity current (e.g., Mied et al., 1996), which imposes a strong constraint of convergence on the buoyant side of the front. This feature may be especially significant in understanding the observed length and time scales. For example, recent work by Cooper et al. (2001) and Mied et al. (in press) simulates the evolution in shape of a gravity current frontal outcrop due solely to nonlinear self-interaction of the front. Although their model does not include the effects of along-front shear, they show that assumed shape and velocity perturbations made to an initial frontal configuration maintain their length scale of several kilometers and grow rapidly within several hours. However, as the perturbations grow the propagation of a frontal element follows an increasingly curved trajectory, which at some point violates the underlying physical assumption of the model and suggests a limit to the amplitude of the cusps.

For the scenario explored by Munk et al. (2000), the hallmark of the instability is an intensifying 'cat's eye' flow pattern that winds any pre-existing slicks into cyclonic spirals that resemble observed ocean spirals. But unlike the larger spiral eddy, we do not observe a spiraling slick pattern. Instead, pre-existing slicks on the Gulf Stream side advect into the front and vanish because of frontal subduction and mixing, while on the shelf-water side of the front slicks appear to grow from the front itself (Fig. 3), subsequently advecting cyclonically around the cusp and then turning inward and reattaching to the front (Fig. 2). In our case, then, the slick extending downstream from a cusp serves to delineate the edge of region of cyclonic motion. The across-front extent of this cyclonic region is of the same order as the amplitude of the frontal cusps, but in the along-front direction it is confined to only the downstream side of a cusp, and this allows the buoyant fluid to advect into the frontal zone on the upstream side of a cusp.

A new feature of the present observations is the growth of slicks in association with the frontal cusps. We propose that the genesis of the slicks begins with an increase in the amount of surfactant on the buoyant side of the front. This increase is mediated through the action of air bubbles that are injected into the water column from the enhanced wave breaking along the front. As the bubbles rise to the surface, they scavenge surface-active organic compounds from the water column through adsorption (e.g., Skop et al., 1994). Bubbles and surfactant may also derive from biological material concentrated by the front. The bubble trajectories in the vertical plane are determined by the rotor circulation and turbulence levels in the frontal head. Material lying near the frontal outcrop will tend to be subducted or mixed into the water column by breaking waves. Some evidence for the 'recycling' of material to the surface is the presence of pieces of *Sargassum* lying between the frontal outcrop and the foam band (Section 3.2) if these were initially submerged by strong sinking motion along the frontal outcrop. The upstream slick and foam band are conjectured to arise then from convergence along the trailing-edge front. The downstream slick arises primarily from advection though current shear and convergence may also play a role. As the downstream slicks are hypothesized to evolve from the foam bands, they tend to have little visible foam due to the finite lifetime of sea foam (Peltzer and Griffen, 1988). The slick patterns thus result from an interplay between the frontal mixing dynamics, which may be thought to act principally in the vertical plane of flow, and the much larger-scale frontal instability dynamics, which act in the horizontal plane.

Finally, one might suspect that along-front variations in density and relative current as sketched in Fig. 7 would give rise to a systematic modulation in the radar signature of the frontal outcrop line. Indeed, for an idealized case where the frontal outcrop line and the relative velocity field have a simple sinusoidal variation, numerical simulations done by Chubb et al. (1999) show significant signal enhancement at the crests and troughs. We believe the resolution of the present radar data set is inadequate to satisfactorily investigate any along-front signal modulation. However, data collected in future studies using synthetic aperture radar systems may have sufficient spatial resolution and signal levels to pursue such questions.

5. Conclusions

A time sequence of airborne microwave radar images and coincident (but limited) in situ data have been used to examine the small-scale structure of a frontal region, which formed through intrusion of relatively dense Gulf Stream water onto the continental shelf. The major results are as follows:

- The frontal outcrop is shown to have a kilometer-wavelength scalloped structure consisting of sharp angular features (cusps) alternating with broad, gently curved regions (troughs). There is also an associated pattern of slicks lying on the buoyant side of the front and asymmetrically offset from the cusps.
- The region included by the cusps contains dense water that subducts at the frontal outcrop while the region within the intervening troughs contains buoyant water. Thus, the sense of the across-frontal density gradient can be inferred directly from the orientation of the cusps in the imagery.
- The slicks appear to originate from processes associated with the front itself. Thus, we believe this is the first published report documenting the genesis of a natural ocean slick.
- Both the frontal scallops and slicks grow to large amplitude (100 to 200 m) in about 1 h and can persist for at least several hours.
- A conceptual model is proposed in which the distinctive horizontal patterns arise from a shear-flow instability modified by the requirement for convergence of buoyant water along the front.
- We conjecture that the presence of convergence velocities of the same order as the along-front velocity shear current changes the frontal instability problem substantially and is responsible for the shorter length scales and growth times we observed.
- The conceptual model suggests the slicks appearing in the radar imagery can be used to characterize certain aspects of the frontal circulation such as the position of a trailing-edge secondary front and the extent of a region of cyclonic circulation.

Additional field measurements and modeling studies will be needed to test our hypotheses. If, as conjectured, the problem includes an interdependent three-dimensional structure, then a complete explanation of the instability and the associated slicks will need to include many effects, ranging from instability dynamics, to smaller-scale frontal circulation, to the micro-scale dynamics of bubbles and surfactant.

Acknowledgements

The field measurements and initial processing that made this study possible were done under the Naval Research Laboratory's High-Resolution Remote Sensing Program. Subsequent analysis was done under PE-61153N (WU 72-5938, WU 72-7815, and WU 72-T090-02). This work is funded by the Office of Naval Research.

References

Alpers, W.R., Ross, D.B., Rufenach, C.L., 1981. On the detectability of ocean surface waves by real and synthetic aperture radar. J. Geophys. Res. 86, 6481–6498.

Britter, R.E., Simpson, J.E., 1978. Experiments on the dynamics of a gravity current head. J. Fluid Mech. 88, 223–240.

Chemi, L., Graber, H.C., Ross, D.B., Shay, L.K., 1993. Fields of ocean surface currents during HIRES-1, Tech. Rep. 93-004, 113 pp., Rosenstiel Sch. of Mar. and Atmos. Sci., Univ. of Miami, Miami, FL.

Chubb, S.R., Cooper, A.L., Jansen, R.W., Fusina, R.A., Lee, J.-S., Askari, F., 1999. Radar backscatter from breaking waves in Gulf Stream current convergence fronts. IEEE Trans. Geosci. Remote Sens. 37, 1951–1966.

Churchill, J.H., Berger, T.J., 1998. Transport of Middle Atlantic Bight shelf water to the Gulf Stream near Cape Hatteras. J. Geophys. Res. 103, 30605–30621.

Cooper, A.L., Mied, R.P., Lindemann, G.J., 2001. The evolution of freely propagating, two-dimensional surface gravity current fronts. J. Geophys. Res. 106, 16887–16901.

Garvine, R.W., 1974. Dynamics of small-scale oceanic fronts. J. Phys. Oceanogr. 4, 557–569.

Garvine, R.W., 1979. An integral hydrodynamic model of upper ocean frontal dynamics: Part 1. Development and analysis. J. Phys. Oceanogr. 9, 1–18.

Garvine, R.W., Monk, J.D., 1974. Frontal structure of a river plume. J. Geophys. Res. 79, 2251–2259.

Jansen, R.W., Shen, C.Y., Chubb, S.R., Cooper, A.L., Evans, T.E., 1998. Subsurface, surface, and radar modeling of a Gulf Stream current convergence. J. Geophys. Res. 103, 18723–18743.

Largier, J.L., 1992. Tidal intrusion fronts. Estuaries 15, 16–39.

Le Fevre, J., 1986. Aspects of the biology of frontal systems. Adv. Mar. Biol. 23, 163–299.

Liu, C., Moncrieff, M.W., 2000. Simulated density currents in idealized stratified environments. Mon. Weather Rev. 128, 1420–1437.

Luketina, D.A., Imberger, J., 1987. Characteristics of a surface buoyant jet. J. Geophys. Res. 92, 5435–5447.

Lyzenga, D.R., 1998. Effects of intermediate-scale waves on radar signatures of ocean fronts and internal waves. J. Geophys. Res. 103, 18759–18768.

Lyzenga, D.R., Marmorino, G.O., 1998. Measurement of surface currents using sequential SAR images of slicks patterns near the edge of the Gulf Stream. J. Geophys. Res. 103, 18769–18777.

Marmorino, G.O., Trump, C.L., 1994. A salinity front and current rip near Cape Hatteras, North Carolina. J. Geophys. Res. 99, 7627–7637.

Marmorino, G.O., Trump, C.L., 2000. Gravity current structure of the Chesapeake Bay outflow plume. J. Geophys. Res. 105, 28847–28861.

Marmorino, G.O., Lyzenga, D.R., Kaiser, J.A.C., 1999. Comparison of airborne synthetic aperture radar imagery with in situ surface-slope measurements across Gulf Stream slicks and a convergent front. J. Geophys. Res. 104, 1405–1422.

Mied, R.P., Shen, C.Y., Evans, T.E., Lindemann, G.J., 1996. Frontogenesis with ageostrophic vertical shears and horizontal density gradients: Gulf Stream meanders onto the continental shelf. J. Geophys. Res. 101, 18079–18104.

Mied, R.P., Cooper, A.L., Lindemann, G.J., Sletten, M.A., in press. Wave propagation along freely propagating surface gravity current fronts. Dyn. Atmos. Ocean.

Munk, W., Armi, L., Fischer, K., Zachariasen, F., 2000. Spirals on the sea. Proc. R. Soc. Lond., A 456, 1217–1280.

Peltzer, R.D., Griffen, O.M., 1988. Stability of a three-dimensional foam layer in seawater. J. Geophys. Res. 93, 10804–10812.

Pingree, R.D., Forster, G.R., Morrison, G.K., 1974. Turbulent convergent tidal fronts. J. Mar. Biol. Assoc. U.K. 54, 469–479.

Samelson, R.M., 1993. Linear instability of a mixed-layer front. J. Geophys. Res. 98, 10195–10204.

Samelson, R.M., Chapman, D.C., 1995. Evolution of the instability of a mixed-layer front. J. Geophys. Res. 100, 6743–6759.

Skop, R.A., Viechnicki, J.T., Brown, J.W., 1994. A model for microbubble scavenging of surface-active lipid molecules from seawater. J. Geophys. Res. 99, 16395–16402.

Sletten, M.A., Marmorino, G.O., Donato, T.F., McLaughlin, D.J., Twarog, E., 1999. An airborne, real-aperture radar study of the Chesapeake Bay outflow plume. J. Geophys. Res. 104, 1211–1222.

Wang, D.P., 1993. Model of frontogenesis: subduction and upwelling. J. Mar. Res. 51, 497–513.